ԵՐԵՎԱՆԻ ՖԻԶԻԿԱՅԻ ԻՆՍՏԻՏՈՒՏ
ЕРЕВАНСКИЙ ФИЗИЧЕСКИЙ ИНСТИТУТ

ЕФИ-676(66)-83

F.A.AHARONIAN, V.G.KIRILLOV-UGRYUMOV, V.V.VARDANIAN

DEVELOPMENT OF HIGH-ENERGY ELECTROMAGNETIC CASCADE INITIATED BY RELATIVISTIC ELECTRONS AND GAMMA-RAYS IN HOT PHOTON GASES

ԵՐԵՎԱՆ 1983 ЕРЕВАН

ЕФИ-676(66)-83

Ф.А.АГАРОНЯН, В.В.ВАРДАНЯН*, В.Г.КИРИЛЛОВ-УГРЮМОВ*

РАЗВИТИЕ ВЫСОКОЭНЕРГИЧНОГО ЭЛЕКТРОМАГНИТНОГО КАСКАДА, ИНИЦИИРУЕМОГО РЕЛЯТИВИСТСКИМИ ЭЛЕКТРОНАМИ И ГАММА-КВАНТАМИ В ГОРЯЧЕМ ФОТОННОМ ГАЗЕ

Обсуждается возможность формирования релятивистских электронно-фотонных ливней в компактных рентгеновских источниках. Приводятся результаты, полученные методом Монте-Карло, по спектральным и временным характеристикам этих ливней.

Ереванский физический институт
Ереван 1983

* Московский инженерно-физический институт

ЕФИ-676(66)-83

F.A.AHARONIAN, V.G.KIRILLOV-UGRYUMOV*, V.V.VARDANIAN*

DEVELOPMENT OF HIGH-ENERGY ELECTROMAGNETIC CASCADE INITIATED BY RELATIVISTIC ELECTRONS AND GAMMA-RAYS IN HOT PHOTON GASES

The possibility of relativistic electron-photon shower formation in compact X-ray sources is discussed. The results of Monte-Carlo calculations are reported.

Yerevan Physics Institute

Yerevan 1983

---

* Moscow Physical Engineering Institute

YEREVAN PHYSICS INSTITUTE

ЕФИ-676(66)-83

F.A.AHARONIAN, V.G.KIRILLOV-UGRYUMOV, V.V.VARDANIAN

DEVELOPMENT OF HIGH-ENERGY ELECTROMAGNETIC CASCADE INITIATED BY RELATIVISTIC ELECTRONS AND GAMMA-RAYS IN HOT PHOTON GASES

Yerevan 1983

1. Introduction

The high luminosities and rapid variabilities of compact X-ray sources testify strongly to enormous density of photons in the production regions. Under such conditions free escaping of hard gamma-rays from the sources, even at their efficient production, is greatly suppressed due to $(e^{+}e^{-})$ photoproduction provided that the essential beaming of radiation is absent. Herterich [1] was the first who stressed the significance of this process in compact galactic X-ray sources. Copious pair production as a result of photon-photon collisions apparently takes place also in the sources of gamma-ray bursts and in the nuclei of active galaxies and quasars (e.g. [2], [3]).

Basing on the observed X-ray fluxes only and supposing that X-rays are approximately isotropically distributed in the source, one may obtain the model-independent upper limit on the production region size R_c at which pair production on X-rays becomes inevitable. Indeed, using the approximate formula for optical depth to photon-photon collisions [1]

$$\tau_{\gamma\gamma} = R \cdot \sigma_0 \cdot n_x(2E_s) \cdot 2{,}5E_s \,, \qquad (1)$$

where $n_x(\omega) \geq \left(\frac{d}{R}\right)^2 \frac{\Phi_x(\omega)}{c}$; $E_s = \frac{2m^2c^4}{E_\gamma}$; $\sigma_o = 1.7 \cdot 10^{-25} cm^2$,

from the condition $\tau_{\gamma\gamma} = 1$ we obtain, e.g. for $E_\gamma = 100$ MeV

$$R_c \geq 6 \cdot 10^5 (d/1\,kpc)^2 [\Phi_x(10\,keV)/10^{-2} cm^{-2} s^{-1} keV^{-1}] cm, \quad (2)$$

where d is the distance to the source and Φ_x (10 keV) is the X-ray flux at the energy $\omega = 10$ keV. Particularly $R_c \sim 2 \cdot 10^8$ cm for Cyg X-1 ($d \simeq 2.5$ kpc and Φ_x (10 keV) $\sim 5 \cdot 10^{-2} cm^{-2} s^{-1}$ keV^{-1}) and $R_c \sim 3 \cdot 10^{17}$ cm for 3C 273 ($d = 860$ Mpc at $H_o = 55$ km/Mpc s) and Φ_x (~ 10 keV) $\sim 6 \cdot 10^{-4} cm^{-2} s^{-1}$ keV^{-1}), respectively.

On the other hand, it follows from the variabilities of these sources that the linear sizes of the 2-10 keV photon production regions do not exceed those values, and hence $\tau_{\gamma\gamma} \geq 1$, if the radiation is not highly beamed. A similar situation takes place in many other compact X-ray sources, both of galactic and extragalactic origin. Thus, if hard gamma-rays are in some way formed in the compact X-ray source, then they interact efficiently with ambient X-ray field before escaping from the source. However the condition $\tau_{\gamma\gamma} > 1$ does not really mean that the source is opaque for gamma-rays. Indeed, one of the secondary electrons produced in the collisions of gamma-rays with ambient X-rays acquires the energy $E_e \sim E_\gamma$ [4]; this electron, scattering then on the same X-rays, produces a high energy photon, the latter gaining approximately the whole energy of the incident electron [5-7]. The processes of bremsstrahlung and annihilation of nonthermalized electrons and positrons may also lead to the formation of high energy gamma-rays [8, 9]. These gamma-rays then interacting with ambient photons again produce (e^+e^-) pairs, and so on. It is obvious that the spectrum of the emerge gamma-radiation will be formed mainly due to the development of

the high-energy electromagnetic cascade in the source.

In this paper we investigate the development of relativistic electron-photon showers in compact X-ray sources.

The dynamics of relativistic cascade showers in hot plasma has been studied by Monte-Carlo technique. When modelling cascade, it was assumed that the plasma-target is stationary, i.e. the plasma perturbations due to relativistic electron- and gamma-ray bombardment were admitted negligible. This assumption is made essentially for all the cases under consideration.

Here we restrict our consideration to nonrelativistic medium, i.e. it's assumed that the mean energy of photons and electrons of plasma is less than mc^2 = 0.5 MeV. Nonthermal particles of electron-photon showers are being traced up to the energy $E \sim 100$ keV, later on it is admitted their "instant" thermalization in the plasma. Evidently the energy carried by those particles into the medium must be less than total inner energy.

In studying the dynamics of electromagnetic cascade, developed in hot plasmas, we took into account the following processes:

- pair production in photon-photon collisions;
- inverse Compton scattering of electrons (positrons) on target photons;
- bremsstrahlung and annihilation of electrons and positrons;
- scattering of suprathermal electrons on the plasma electrons (Møller and Bhabha scattering);
- Compton scattering and (e^+e^-) pair production by gamma-rays on the electrons and nuclei of plasma;
- synchrotron energy losses of relativistic electrons.

In the radiation-dominated plasma ($P_{rad} > P_{gas}$) the first two processes play the main role in the cascade development, though the interactions with

ambient thermal electrons (especially the annihilation of thermalized positrons) also become essential in forming the gamma-ray spectrum in the low-energy ($\sim mc^2$) region.

Consider now the microscopic processes responsible for the cascade development in hot plasmas.

2. Interaction Processes

A. Pair Production in Photon-Photon Collisions.

The total cross section of the process is determined by expression (e.g. [10])

$$\sigma_{pp} = \frac{1}{2}\pi r_0^2 (1-\beta_0^2)\beta_0 \left[\frac{(3-\beta_0^4)}{\beta_0} \ln\frac{1+\beta_0}{1-\beta_0} + 2(\beta_0^2-2)\right], \qquad (3)$$

where $r_0^2 = e^2/mc^2$ is the classical radius of the electron, $\beta_0 = v/c$ is the velocity of the electron (positron) in the centre-of-momentum (c.m.) frame *.

Let E_γ and ω be the energies of the two colliding photons, and θ be the angle of collision. The relation between E_γ , ω , β_0 and θ can be found from the condition of relativistic invariance of the total four-momentum:

$$2\omega E_\gamma (1-\cos\theta) = 4E_0^2 \; ; \quad E_0 = (1-\beta_0^2)^{-1/2} , \qquad (4)$$

where E_0 is the electron (positron) energy in the c.m.-frame.

The probability of gamma-ray absorption on the unit length when passing through isotropically distributed photon gas with density $n(\omega)$ is

---

* In the following for simplicity we take $c = \hbar = m = 1$.

$$\frac{d\tau_{pp}}{dx} = \frac{1}{2}\int\int \sigma_{pp}\, n(\omega)(1-\cos\theta)\sin\theta\, d\theta\, d\omega. \qquad (5)$$

Introducing $s = \frac{1}{2}\omega E_\gamma (1-\cos\theta)$ and passing from the integration over θ to the integration over s one obtains

$$\frac{d\tau_{pp}}{dx} = \frac{\pi r_0^2}{E_\gamma^2}\int_{1/E_\gamma}^{\infty} \omega^{-2}\, n(\omega)\, \varphi(s_0(\omega))\, d\omega, \qquad (6)$$

where

$$\varphi(s_0(\omega)) = \int_1^{s_0(\omega)} s\,\bar{\sigma}(s)\, ds\,; \quad \bar{\sigma}(s) = \frac{2\sigma_{pp}(s)}{\pi r_0^2}\,; \quad s_0 = \omega E_\gamma \qquad (7)$$

Analytical integration of Eq. (7) has been performed by Gould and Schreder [11]. The asymptotic expressions for the function $\varphi(s_0)$ have a form

$$\varphi(s_0) = 2s_0(\ln 4s_0 - 2) + \ln 4s_0\,(\ln 4s_0 - 2) - \frac{\pi^2 - 9}{3} + \qquad (8a)$$
$$+ s_0^{-1}(\ln 4s_0 + 9/8) + \ldots \qquad s_0 \gg 1\,;$$

$$\varphi(s_0) = \frac{2}{3}(s_0-1)^{3/2} + \frac{5}{3}(s_0-1)^{5/2} - (1507/420)(s_0-1)^{7/2}, \qquad (8b)$$
$$s_0 - 1 \ll 1.$$

The differential cross section of the process can be written as (e.g. [10])

$$d\sigma_{pp} = \frac{r_0^2}{4}(1-\beta_0^2)\,\beta_0\, U_0\, d\Omega^*, \qquad (9)$$

where

$$U_o = \frac{1+2\beta_o^2\sin^2\theta^* - \beta_o^4(1+\sin^4\theta^*)}{(1-\beta_o^2\cos^2\theta^*)^2} ,$$

θ^* is an angle between vectors $\vec{K}$ and $\vec{P}$ in the c.m.-frame; $\vec{P}$ is the momentum of one of the electrons.

The energies of the produced electrons in the laboratory (L) frame are equal to

$$E_\pm = \gamma_c \omega (1 \pm \beta_c \beta_o \cos\theta^*) , \qquad (10)$$

and the emission angles relative to total momentum $\vec{K}_1 + \vec{K}_2$ are

$$\theta_\pm = \operatorname{arctg}\left[\frac{\sin\theta^*}{\gamma_c(\beta_c/\beta_o \pm \cos\theta^*)}\right] \qquad (10')$$

Here

$$= \frac{|\vec{K}_1 + \vec{K}_2|}{E_\gamma + \omega} , \qquad \gamma_c = (1-\beta_c^2)^{-1/2}$$

The spectrum of the secondary electrons and positrons in the case of isotropic and monoenergetic field of low-energy photons ($\omega \ll 1$) has the form [4] :

$$\frac{dN}{dE_e} = \frac{\pi r_o^2}{4\omega^2 E_\gamma^3}\left[\frac{4E^2}{(E-E_e)E_e}\ln\frac{4\omega(E-E_e)E_e}{E} - \right. \qquad (11)$$

$$\left. - 8\omega E + \frac{2(2\omega E-1)E^2}{(E-E_e)E_e} - (1-1/\omega E)\frac{E^4}{(E-E_e)^2 E_e^2}\right],$$

where $E_e \equiv E_\pm$, $E \simeq E_\gamma$. The variation range of E_e is determined from the kinematics of the reaction

$$\frac{E}{2}\left(1-\sqrt{1-\frac{1}{\omega E}}\right) \leq E_e \leq \frac{E}{2}\left(1+\sqrt{1-\frac{1}{\omega E}}\right).$$

The electron spectrum is symmetric relative to energy $\frac{E_\gamma+\omega}{2}$. In the case of $E_\gamma \neq \omega$ this point corresponds to the minimum of the spectrum, the spectrum displaying two strong maxima, symmetric with respect to the minimum. At $E_\gamma \to \omega$ the maxima approach each other and in the case of $E_\gamma = \omega$ fuse together, bringing to the logarithmical divergency of the spectrum, which does not however lead to the divergency of the total cross section [4].

The spectrum shape depends strongly on the parameter $S_0 = \omega E_\gamma$. At $S_0 - 1 \leq 1$ the secondary electrons have a flat spectrum. If $S_0 \gg 1$, the maxima become more expressive, one of the electrons gaining approximately the whole energy of the high-energy gamma-quantum ($E_e \sim E_\gamma$) [4]. The spectrum of produced electrons evidently can be smoothed, if the field photons have some broad distribution function $n(\omega)$. The Monte-Carlo simulation of the pair characteristics for arbitrary distribution of field photons $n(\omega)$ based on the cross section (9) and kinematic relationship (10) is described in the Appendix.

B. Compton Effect.

The total cross section of the Compton scattering of the photon with energy ω and the electron with energy E_e in the L-frame is equal to (e.g. [10])

$$\sigma_c = \frac{2\pi r_0^2}{\chi_1}\left[(1-4/\chi_1-8/\chi_1^2)\ln(1+\chi_1)+1/2+8/\chi_1-1/2(1+\chi_1)^2\right], \quad (12)$$

where $\chi_1 = 2\omega E_e(1-\beta\cos\theta)$; θ is the scattering angle and β is the electron velocity in the L-frame.

The probability of the electron collision on the unit length passing

trough isotropically distributed photon gas with density $n(\omega)$ is

$$\frac{d\tau_c}{dx} = \frac{1}{\beta}\int\int \frac{1}{2}\sigma_c n(\omega)(1-\beta\cos\theta)\sin\theta d\theta d\omega.$$

Changing variable integration for θ by x_1 one obtains

$$\frac{d\tau_c}{dx} = \frac{\pi r_o^2}{\beta^2}\left(\frac{1}{2E_e}\right)^2\int_0^\infty \omega^{-2} n(\omega)\varphi(x_{10}(\omega))d\omega, \qquad (13)$$

where

$$\varphi(x_{10}(\omega)) = \int_{x_{10}(1-\beta)}^{x_{10}(1+\beta)} x_1 \bar{\sigma}_c(x_1)dx_1;$$

$$\bar{\sigma}_c(x_1) = \sigma_c(x_1)/2\pi r_o^2; \qquad x_{10} = 2\omega E_e.$$

After integration over x_1 for $\varphi(x_{10})$ we have

$$\varphi(x_{10}) = F(1+\beta) - F(1-\beta) - x_{10}\beta - 4\int_{x_{10}(1-\beta)}^{x_{10}(1+\beta)} \frac{\ln(1+x_1)}{x_1}dx_1, \qquad (14)$$

$$F(z) = \ln(1+x_{10}z)(x_{10}z+9+8/x_{10}z) + 0.5/(x_{10}z+1).$$

The differential cross section of the process can be expressed through relativistic invariants $x_1 = 2\omega_o(E_o+\omega_o)$ and $x_2 = 2\omega_o(E_o+\omega_o\cos\theta^*)$ (e.g. [10]):

$$d\sigma_c = r_o^2 \frac{2\omega_o^2}{x_1} u_o d\Omega^*, \qquad (15)$$

where

$$u_o = \frac{x_1}{x_2} + \frac{x_2}{x_1} + 4\left(\frac{1}{x_2} - \frac{1}{x_1}\right) + 4\left(\frac{1}{x_2} - \frac{1}{x_1}\right)^2;$$

ω_o and $E_o = (\omega_o^2 + 1)^{1/2}$ are energies of photon and electron and θ^* is the angle between momenta $\vec{K}$ and $\vec{K}'$ in the c.m.-frame.

Relationship between ω_o and particles parameters in the L-frame is determined from the condition $(P+K)^2 = inV$:

$$\omega_o = \frac{x_1}{2\sqrt{1+x_1}}$$

The energies and emission angles (relative to total momentum) of photon and electron in the L-frame after scattering are

$$\omega' = \gamma_c \omega_o (1 - \beta_c \cos\theta^*), \qquad (16)$$
$$E_e' = \gamma_c \omega_o (1 + \beta_c \beta_o \cos\theta^*);$$

$$\theta_\gamma = \operatorname{arctg}\left[\frac{\sin\theta^*}{\gamma_c(\beta_c - \cos\theta^*)}\right], \qquad (17)$$

$$\theta_e = \operatorname{arctg}\left[\frac{\sin\theta^*}{\gamma_c(\beta_c/\beta_o + \cos\theta^*)}\right],$$

where

$$\beta_c = \frac{|\vec{P}_i + \vec{K}_i|}{Ee + \omega}, \quad \gamma_c = (1-\beta_c^2)^{-1/2}; \quad \beta_o = \omega_o / E_o.$$

In the case of the inverse Compton scattering ($E_e - 1 \gg \omega$) of relativistic electrons on the isotropically distributed photon field the spectrum of single scattered photons essentially depends on parameter $\beta = 4\omega E_e$. At $\beta \ll 1$ the spectrum monotonously decreases with increasing energy of scattered photon [12]. In the opposite limit ($\beta \gg 1$) a strong rise of the spectrum is revealed near the upper kinematic edge

$\left(\omega \sim \omega_{max} \approx \frac{\beta E_e}{1+\beta}\right)$, i.e. after the single scattering high-energy photon is produced, the latter gaining approximately the whole energy of the relativistic electron [5-7].

The cross section of the process becomes essentially simplier when high-energy photons are scattered by nonrelativistic electrons, i.e. the condition $E_e - 1 \ll \omega$ (direct Compton scattering) holds. Particularly, the total cross section is described by Eqs.(12) with $\chi_1 = 2\omega$ ($\beta \approx 0$; $E_e \approx 1$) and the differential cross section is

$$d\sigma_c = \pi r_0^2 \frac{d\omega'}{\omega^2}\left[\frac{\omega}{\omega'} + \frac{\omega'}{\omega} + \left(\frac{1}{\omega'} - \frac{1}{\omega}\right)^2 + 2\left(\frac{1}{\omega'} - \frac{1}{\omega}\right)\right] \tag{18}$$

where $E' = \omega^2(1-\cos\theta_\gamma)/\left[1+\omega(1-\cos\theta_\gamma)\right] + 1$,

and ω' varies within the limits $\omega/(1+2\omega) \le \omega' \le \omega$.

The scattering angles of photon and electron are respectively

$$\theta_\gamma = \operatorname{arctg}(1 - 1/\omega' - 1/\omega) \tag{19}$$

$$\theta_e = \operatorname{arctg}\left[(1+\omega)\sqrt{\frac{1-\cos\theta_\gamma}{2+\omega(\omega+2)(1-\cos\theta_\gamma)}}\right]$$

The Monte-Carlo simulation of parameters of scattered electrons and photons for arbitrary initial distributions is described in the Appendix.

C. Annihilation of Electron-Positron Pairs.

The total cross section of free annihilation of an electron-positron pair (neglecting the formation of positronium prior to annihilation) into two photons is (e.g. [10])

$$\sigma_a = \pi r_0^2 \frac{1-\beta_0^2}{4\beta_0}\left[\frac{3-\beta_0^2}{\beta_0}\ln\frac{1+\beta_0}{1-\beta_0} + 2(\beta_0^2-2)\right], \qquad (20)$$

where $\beta_0 = \sqrt{\frac{E_+ - 1}{E_+ + 1}}$, E_+ is the positron energy in the rest frame of the electron.

The differential cross section of the process in the c.m.-frame may be expressed in the form (e.g. [10])

$$d\sigma_a = \frac{r_0^2}{4}\frac{1-\beta_0^2}{\beta_0} u_0 \, d\Omega^* \qquad (21)$$

where

$$u_0 = \frac{1 + 2\beta_0^2 \sin\theta^* - \beta_0^4(1+\sin^4\theta^*)}{(1-\beta_0^2\cos^2\theta^*)^2},$$

θ^* is the angle between $\vec{P}_+$ and $\vec{K}$, and β_0 is the velocity of electron (positron) in the c.m.-frame.

Energies and angles of emitted annihilation photons relative to the direction of initial positron in the rest frame of electron are

$$\omega_{1,2} = \frac{E_+ + 1}{2}\left(1 \pm \beta_0 \cos\theta^*\right)$$

$$\theta_{1,2} = \operatorname{arctg}\left[\frac{\sin\theta^*}{\gamma_c(\beta_0 \pm \cos\theta^*)}\right], \qquad (22)$$

where $\gamma_c = (1-\beta_0^2)^{-1/2}$

In the general case the method for Monte-Carlo simulation of parameters of annihilation photons for arbitrary distributions of electrons is described in the Appendix.

In the case of rest electrons, i.e. when suprathermal positrons are injected in cold medium ($E_+ \gg KT \ll 1$), annihilation takes place both

before and after thermalization of positrons. Annihilation of suprathermal positrons leads to continuous spectrum of photons [8, 9]

$$\frac{dN}{d\omega} = \frac{\pi r_0^2}{E_+ P_+}\left[2\left(\frac{1}{\omega} + \frac{1}{E_+ + 2 - \omega}\right) - \left(\frac{1}{\omega} + \frac{1}{E_+ + 1 - \omega}\right)^2 + \right.$$

$$\left. + \left(\frac{\omega}{E_+ + 1 - \omega} + \frac{E_+ + 1 - \omega}{\omega}\right)\right]; \qquad (23)$$

$$\frac{1}{2}(E_+ + 1 - P_+) \leq \omega \leq \frac{1}{2}(E_+ + 1 + P_+),$$

where P_+ and E_+ are initial momentum and energy of annihilating positron in the L-frame.

The spectrum (23) displays two strong maxima symmetric with respect to the point of minimum $\omega_{min} = \frac{E_+ + 1}{2}$. The maxima are reached near two edges of kinematic range (23). In the case of annihilation of relativistic positrons ($E_+ \gg 1$) with rest electrons the maxima are reached in the points $\omega = 0{,}5$ and $\omega = E_+ + 0{,}5$, i.e. one of the annihilation photons gains approximately the whole energy of the positron.

However only small portion of relativistic positrons manage to annihilate before thermalization. Due to ionization, Compton and synchrotron energy losses the main part of positrons annihilate after thermalization in the medium. As a result, the 0.511 line and perhaps 3-photon continuum of positronium are formed. The annihilation spectrum formed in cold medium ($T \leq 10^6$K) has been considered in detail by Ramaty and co-workers [13,14] In the hot plasma ($T \gg 10^6$K) (e^+e^-) pairs annihilate mainly in the free state before the formation of positronium.

Annihilation spectrum of hot Maxwellian plasmas has been recently calculated by a number of authors. In two extreme limits the radiation spectrum may be expressed in a simple analytical * form [15, 16]

* Hereafter we use the physical constants m and C explicitly.

$$\frac{dN}{d\omega} = n_+ n_- \frac{2\sqrt{\pi} r_0^2 c}{mc^2\sqrt{\theta}} \left(1 + \frac{3}{2}\Delta\right) e^{-\Delta^2/\theta} \qquad \theta\omega \ll mc^2 \qquad (24)$$

and

$$\frac{dN}{d\omega} = n_+ n_- \frac{\pi r_0^2 c}{2\theta^4} \left(\ln \eta_E \theta - 1\right) \frac{\omega}{mc^2} e^{-\omega/\theta mc^2} \qquad \theta\omega \gg mc^2 \qquad (25)$$

$$(\eta_E = 0{,}5616; \quad \Delta = \omega/mc^2 - 1; \quad \theta = KT/mc^2).$$

At low temperatures ($KT \ll mc^2$) the spectrum has a maximum at $\omega_{max} = mc^2 + 3/4\, KT$, the mean energy of photons being equal to $\langle\omega\rangle = mc^2 + 3/2\, KT$. The FWHM of the line is equal to $2\sqrt{\ln 2} \times \theta^{1/2} mc^2$.

At relativistic temperatures ($KT \gg mc^2$) the maximum of spectrum is at $\omega_{max} = mc^2 + 1{,}2\, KT$; the mean energy of photons is equal to $\langle\omega\rangle = mc^2 + 2KT$, and FWHM $\simeq 2.5\ KT$.

D. Pair Production by Gamma-Rays, Bremsstrahlung and Scattering of Electrons and Positrons in the Gases.

A lot of reviews are devoted to these processes. Since here we examine the development of the electromagnetic cascade in nonrelativistic plasmas we may assume that the plasma's electrons and ions are in rest. Therefore we may use well-developed methods applied for simulating electromagnetic cascade showers in the gases. Here we applied the simulation methods suggested by Messel and Crawford [17]. In the calculations catastrophic events were considered to be only those at which the energy of the secondary products of reactions (knock-on electrons; bremsstrahlung photons) exceeded 100 keV. For the lower energies of secondaries continuous energy losses due to bremsstrahlung and $e^+ - e^-$ and $e^- - e^-$ scatterings have been introduced.

E. Synchrotron Radiation.

A more important process, connected with interactions of charged particles with moderate magnetic fields, is the synchrotron radiation of electrons. The spectrum of the radiation has an asymmetrical shape with maximum at the energy

$$\omega = 5 \cdot 10^{-9} \left(E_e / mc^2 \right)^2 H_\perp \text{ eV}$$

where in the case of chaotic fields $H_\perp^2 = \frac{2}{3} H^2$.

Hence, X- and gamma-rays can be efficiently produced due to this process only at extreme magnetic fields and electron energies. That is why in calculations this process as well as the Compton scattering of relativistic electrons on the low-frequency (optical, radio) photons have been treated from the point of view of energy losses of electrons. For the rate of continuous (noncatastrophic) energy losses we used the well-known formula [12]

$$\frac{dE}{dt} = \frac{32}{9} \pi r_0^2 c W_{EM} \left(E_e / mc^2 \right)^2 , \qquad (26)$$

where $W_{EM} = W_r + H^2 / 8\pi$ is the summary energy density of magnetic field and low-frequency photons.

3. Results

The most important parameter characterizing development of electromagnetic cascade initiated by relativistic electrons and/or gamma-rays in photon gas is the optical deoth to photon-photon collisions. Evidently at $\tau_{\gamma\gamma} < 1$ the region is transparent for gamma-rays and hence the efficiency of electron-photon shower formation is negligible.

In Figs.1a,b,c the escaping spectra of gamma-rays from the active re-

gion normalized per incident particle are presented assuming that spherical region is isotropically and homogeneously filled with the monoenergetic X-ray photons and density of initiating cascade monoenergetic and isotropic gamma-rays reduces with increasing the radius as r^{-2}. The last assumption is inessential, especially at $\tau_{\gamma\gamma} \gg 1$. It can be seen from the comparison of Figs.1a and 1b with Fig.2, which corresponds to the case, when the initiating gamma-rays are produced in point source, located in the centre of spherical X-ray photon cloud.

The spectra in Figs.1a,b,c correspond to the values of optical depths $\tau_{\gamma\gamma} = n_x \cdot R \cdot \bar{\sigma}_{\gamma\gamma}$: 1, 10 and 100, respectively (n_x is the density of ambient X-rays, R is the radius of the active region, and $\sigma_{\gamma\gamma}$ is the total pair production cross section, averaged over 4π. It was assumed that the plasma particle density is essentially less than the photon density in active region of cascade development. Due to general symmetry of the region the results depend only on the product $n_x R$. From Fig.1a ($\tau_{\gamma\gamma} = 1$) it follows that approximately half of the initial gamma-rays escape freely from the region. The rest lead to the production of secondary photons, electrons and positrons, ~ 10% of initial energy being released in photons, and ~40% in electrons and positrons. The spectrum of escaping photons essentially depends both on ambient X-ray energy ω_o and on initial gamma-ray energy.

The escaping gamma-ray spectrum is standardized when increasing the optical depth $\tau_{\gamma\gamma}$. Indeed, at $\tau_{\gamma\gamma} = 10$ (Fig.1b) the power-law spectrum of secondary photons in the range of $E_\gamma \leq E_c = 2m^2c^4/\omega_o$ (E_c being the threshold of photoproduction corresponding to $\langle \cos\theta \rangle = 0$) is formed, practically independent of initial energy of photon; above the energy E_c the spectrum is steepening and further on it becomes somewhat harder due to escaping of high-energy gamma-rays produced on periphery of the active re-

gion. More than 70% of initial gamma-ray energy is transformed into secondary photons with the energy $\leq E_c$, for which the source is transparent. and approximately 15-20% transformed into escaping relativistic electrons and positrons. The calculations show that the results depend weakly on the source geometry and initial spectrum of gamma-rays. It's interesting to note that the similar results are obtained also in the case when the cascade is initiated by relativistic electrons.

The spectrum of secondary photons comes to complete standard at extreme values of the optical depth $\tau_{\gamma\gamma}$. This is seen from Fig.1c which corresponds to $\tau_{\gamma\gamma} = 100$. The energy spectra have power-law behaviour with power index $\Gamma \simeq 1.5$ up to the energy E_c and cut-off sharply at $E_\gamma \geq E_c$. At such great values of $\tau_{\gamma\gamma}$ the most efficient production of positrons and electrons takes place: $\sim$ 2 pairs per one initiating particle with $E_o = 200 mc^2$, and $\sim$ 20 pairs for $E_o = 2000 mc^2$. Due to Compton energy losses, only the negligible part of these electrons ($\sim 0.1\%$) escape through the active region having relativistic energies, and their luminosity is not greater than $\sim$ 1% of the gamma-ray one. These results have simple physical explanation. Indeed, at $\tau_{\gamma\gamma} \gg 1$, the maximum number of electron-positron pairs produced by a single initiating particle is equal to $K \sim E_o / E_c = E_o \omega_o / m^2 c^4$, where E_o is the energy of initiating particle, ω_o is the field photon energy. At $E_o = 200 mc^2$ and $E_o = 2000 mc^2$ one finds $K \sim 2$ and ~ 20, respectively, ω_o being equal to $0.02\ mc^2$.

The production and escape of relativistic electrons comes to be most efficient at $\tau_{\gamma\gamma} \sim 1 \div 10$. The escaping electron spectra for the values of $\tau_{\gamma\gamma} = 1$ and $\tau_{\gamma\gamma} = 10$ are presented in Fig.3. Whereas at $\tau_{\gamma\gamma} \sim 1$ the escaping electron spectrum is practically the same as the electron production one, for greater values of $\tau_{\gamma\gamma}$ the power-law spectrum is formed

due to Compton scatterings. For example, at $\tau_{\gamma\gamma} = 10$ the electron energy spectrum is well approximated throughout the wide energy range by power-law with $\Gamma \simeq 1.8$. As was mentioned, the relativistic electron luminosity, as distinct from the gamma-ray one, reduces with increasing the optical depth $\tau_{\gamma\gamma}$. Such an anticorrelation is generally explained by the thresholdless feature (unlike the pair production process) of the Compton scattering.

So far we assumed that the active region of cascade development is filled up mainly with X-ray photons and neglected interactions of relativistic particles with plasma electrons and ions. The main parameter, characterizing these interactions is an optical depth of plasma for Thomson scattering $\tau_{es} = n_e \cdot R \cdot \sigma_T$. It is obvious that at moderate values of τ_{es} the interactions with the plasma photons play the crucial role in the cascade development as before, though the interactions with ambient thermal electrons (especially the annihilation of thermalized positrons) also become essential in forming the gamma-ray spectrum in the low-energy ($\sim mc^2$) region.

The spectra of escaping gamma-rays for $\tau_{\gamma\gamma} = 10$ and $\tau_{es} = 1$ are shown in Fig.4. It was also assumed that field photons are monoenergetic with $\omega_o = 0{,}02\, mc^2$ and temperature of plasma in the active region is 30 keV. It should be noted that these assumptions have illustrative character only, however, as follows from the calculations, more realistic and consistent assumptions on plasma parameters (taking into account thermal balance between plasma photons and electrons) lead to approximately similar results.

The distinctive feature of escaping gamma-ray spectrum in this case is the presence of the broad maximum at $E_\gamma \sim (1-2)mc^2$, associated with the annihilation of thermalized positrons. Approximately 25% of the energy of initiating particles and respectively $\sim 45\%$ of energy of escaping gamma-rays is released in this broad "line". It should be noted, however, that the

spectrum in Fig.4 was obtained on the assumption that thermalized positrons annihilate "instantly". In fact, the production of annihilation photons is somewhat delayed owing to finite annihilation time. Indeed, in nonrelativistic plasma the characteristic time of annihilation is $t_{an} \simeq (\pi r_e^2 c n_e)^{-1} = 8R/3\tau_{es}c$, therefore only at $\tau_{es} \geq 3$ the annihilation time becomes less than mean time of photon escape from the active region $\sim R/c$. Thus the photon spectrum in Fig.4 is generally correct only in the case of stationary bombardment of plasma-target by relativistic particles. If the radiation is a result of some "burst", then it is necessary to take into account the real times of photon production and propagation from the active region.

It should be noted also that the escape time for the photons with energies $E_\gamma > E_c$ is less than that for $E_\gamma \leq E_c$. Indeed, only those photons with $E_\gamma > E_c$ may easily escape from the source which are produced in the periphery of the active region, i.e. in the thin external layer with the thickness $\Delta R \sim 1/n_x \bar{\sigma}_{\gamma\gamma}$. Therefore the escape time of these photons, equal by the order of magnitude to $t \sim \frac{\Delta R}{c} \sim \frac{R}{c}\tau_{\gamma\gamma}^{-1}$ *, is $\tau_{\gamma\gamma}$ times less than that for $E_\gamma < E_c$. The accurate calculations of the times of photon escape for various energy ranges, presented in Fig.5, are in good agreement with this simplified estimate. It should be emphasized that the escaping from the transparent outer layer gamma-rays, are secondary products of the photons of various "generations", produced through the whole track of escape. The input from the photons of different "generations" essentially depends on the distribution of initial particles in the active region. Particularly, in the case of the point source located at the centre

---

* Strictly speaking, this simplified estimation is correct for initiating gamma-ray density dependence on the radius r^{-2}.

of X-ray cloud with $\tau_{\gamma\gamma} \gg 1$ all escaping photons are of the secondary origin. In this case the differences of escape times of gamma-rays with various energies are compensated by the shift of their production times and therefore all photons (except the thermal annihilation ones) emerge from the source almost simultaneously for the time $\sim R/c$ after injection of initiating particles, the radiation transfer effects for relativistic particles being inessential. Thus, at $\tau_{\gamma\gamma} = 10$ the photons with energies $0.2\, mc^2 \leqslant E_\gamma \leqslant E_c$ escape from the active region during the time $\sim 1.13\, R/c$. It is due to the fact that the photons are generally propagated in the direction of initiating particles, and hence they "delay" only at $0.13\ R/c$.

All the above calculations are performed under assumption that the magnetic field in the active region is absent, and the density of low-frequency (optical, radio) radiation is negligible. Evidently this admission is correct if synchrotron and Compton losses on low-frequency photons are substantially less than the Compton energy losses on X-rays:

$$\left(\frac{dE}{dt}\right)_X = \pi r_0^2 c \left(\frac{\omega_0}{mc^2}\right)^{-2} W_X \left[\ln \beta - 11/6\right], \tag{27}$$

where W_X is energy density of X-rays. $(= n_X \cdot \omega_0)$.

From the comparison of (26) and (27) we find

$$\left(\frac{dE}{dt}\right)_{EM} \Big/ \left(\frac{dE}{dt}\right)_X \simeq \frac{32}{9} \frac{W_{EM}}{W_X} \left(\frac{\omega_0}{mc^2}\right)^2 \left(\frac{Ee}{mc^2}\right)^2 \left[\ln \beta - 11/6\right]^{-1}.$$

Thus, we may neglect synchrotron and Compton losses on the low-frequency radiation provided

$$\frac{W_X}{W_{EM}} > 0{,}2\beta^2 / \left[\ln \beta - 11/6\right]; \qquad \beta = 4 E e \omega_0 / m^2 c^4. \tag{28}$$

Particularly, for $\omega_o = 10$ keV and $E_e = 100$ MeV $W_X/W_{EM} \geq 10^2$.

Otherwise, the development of the cascade will strongly be suppressed due to synchrotron and Compton (noncatastrophic) losses.

So far we have been discussing the cascade development in monoenergetic X-ray field in order to perceive obviously the results. Though the true spectra of field photons smoothen slightly these results, the obtained features of cascade development remain valid. The formation of electron-photon showers in the real astrophysical objects is considered in our next paper. Relativistic electron-photon showers initiated in outer layers of accretion disks around massive black holes were considered earlier by Burns and Lovelace [18].

The authors are thankful to A.M.Atoyan for valuable discussions.

APPENDIX

A.1. Simulation of Compton Scattering of Relativistic Electrons.

The characteristics of secondaries after Compton scattering in the L-frame are unambiguously defined by the scattering angle θ^* in the c.m.-frame (cf. Sec.2). The frequency distribution for $x = \cos\theta^*$ is

$$P_K(x) = \frac{d\sigma_c/dx}{\sigma_c} = \frac{4\pi r_o^2}{\chi_1^2 \sigma_c}\omega_o u_o . \qquad (A.1)$$

It is convenient to present (A.1) in the form (e.g. [19])

$$P(x) = A f(x) g(x),$$

where A is a constant, $f(x)$ is some finite and smoothly varying function, and

$$\int_{-1}^{1} g(x)dx = 1$$

It is advisable (from the viewpoint of calculation efficiency) to perform the simulation of x by two ways according to the value of invariant $\chi_1 = 2\omega E(1-\beta\cos\theta)$; the energy ω_o and collision angle θ are defined beforehand by simulating the parameters of photon field.

1. Let $g(x) = 0.5$ and $A = \frac{8\pi r_o^2 \omega_o^2}{\chi_1^2 \sigma_c}$. Then $f(x) = u_o$.

Since inequality $f(x) \le 2(\omega_o + E_o)$ takes place, the random variable may be chosen by:

a) select two random uniform numbers within the range (0.1): r_1 , r_2 ;

b) determine $x_o = 2r_1 - 1$;

c) calculate $f(x_o)$ and accept $x = x_o$ provided

$$r_2 \le f(x_0)/2(\omega_0 + E_0)\ ;$$

if rejected, repeat anew with item a)

2. Let

$$g(x) = \frac{1}{(1+\omega_0 x/E_0)(E_0/\omega_0 \ln[(1+\omega_0/E_0)/(1-\omega_0/E_0)])}\ ;$$

$$A = \frac{2\pi r_0^2}{\chi_1 \sigma_c} \ln\left(\frac{1+\omega_0/E_0}{1-\omega_0/E_0}\right).$$

Then

$$f(x) = u_0 \frac{\chi_1}{\chi_2} < 2.$$

In this case preliminary sampling of x is performed by formula

$$x_0 = \left[\frac{(1+\omega_0/E_0)^{r_1}}{(1-\omega_0/E_0)^{r_1}-1}\right]\frac{E_0}{\omega_0}\ ,$$

and this value is accepted if

$$r_2 \le f(x_0)/2.$$

The efficiency of the first procedure is equal to

$$\epsilon_I = \chi_1 \sigma_c / 8\pi r_0^2 \omega_0\ ,$$

and of the second one

$$\epsilon_{II} = \chi_1 \sigma_c / 4\pi r_0^2 \ln\left(\frac{1+\omega_0/E_0}{1-\omega_0/E_0}\right).$$

At $\chi_1 \ll 1$ ϵ_I and ϵ_{II} approach 2/3 $\left(\sigma_c \to \sigma_T = \frac{8}{3}\pi r_0^2\right)$, and at $\chi_1 \gg 1$ ϵ_I approaches 0 as $\ln \chi_1/\chi_1$, and ϵ_{II} approaches 0.5 $\left(\sigma_c \to 2\pi r_0^2 \ln \chi_1/\chi_1\right)$. The efficiencies of the two methods become equal at $\chi_1 \le 1$

A.2. Simulation of Pair Production and Annihilation Processes.

The characteristics of secondaries produced in the processes of pair photoproduction (PP) and annihilation (A) are defined by the emission angle θ^* in the c.m.-frame. The frequency distributions for $x = \cos\theta^*$ for PP and A are respectively

$$P_{PP}(x) = \frac{d\sigma_{PP}/dx}{\sigma_{PP}} = \frac{\pi r_o^2}{2} \frac{\beta_o}{\sigma_{PP}\omega_o} u_o , \qquad (A.2)$$

$$P_a(x) = \frac{d\sigma_a/dx}{\sigma_a} = \frac{\pi r_o^2}{2} \frac{1}{\sigma_a \varepsilon_o^2 \beta_o} u_o . \qquad (A.3)$$

Simulation of x, as in the case with Compton scattering, was performed in two ways according to the value of β_o, which equals to $\frac{(\omega_o^2-1)^{1/2}}{\omega_o}$ and $\frac{(\varepsilon_o^2-1)^{1/2}}{\varepsilon_o}$ for PP and A, respectively. For PP the energy ω_o and collision angle θ are obtained beforehand by simulating the parameters of photon field.

1. Let $g(x) = 0.5$ and $A_{PP} = \frac{\pi r_o^2 \beta_o}{\sigma_{PP}\omega_o^2}$, $A_a = \frac{\pi r_o^2}{2\sigma_a \varepsilon_o^2 \beta_o}$ for PP and A, respectively. Then $f(x) = u_o < \frac{1+\beta_o^2}{1-\beta_o^2}$. The preliminary sampling of x is performed by formula $x_o = 2r_1 - 1$, and this value is accepted if $r_2 < f(x_o)/\left(\frac{1+\beta_o^2}{1-\beta_o^2}\right)$

2. Let $g(x) = \frac{\beta_o}{(1-\beta_o^2 x^2)\ln\frac{1+\beta_o}{1-\beta_o}}$ and $A_{PP} = (\pi r_o^2/2\sigma_{PP}\omega_o^2\beta_o)\ln\frac{1+\beta_o}{1-\beta_o}$ and $A_a = (\pi r_o^2/2\sigma_a\varepsilon_o^2\beta_o^2)\ln\frac{1+\beta_o}{1-\beta_o}$. Hence $f(x) \le 2(\sqrt{2}-1)(\beta_o^2+\sqrt{2})$

The preliminary sampling of x is performed by formula

$$x_0 = \frac{1 - \left(\frac{1+\beta_0}{1-\beta_0}\right)^{2r_1-1}}{\beta_0\left[1 + \left(\frac{1+\beta_0}{1-\beta_0}\right)^{2r_1-1}\right]},$$

and this value is accepted if $r_2 < f(x_0)/(2(\sqrt{2}-1)(\beta_0^2+\sqrt{2}))$

The efficiencies of the first method are equal to

$$\epsilon_I^{pp} = \frac{6_{pp}\omega_0^2}{\pi r_0^2 \beta_0 (1+\beta_0^2)/(1-\beta_0^2)}, \qquad \epsilon_I^{a} = \frac{26_a \beta_0 \varepsilon_0^2}{\pi r_0^2 (1+\beta_0^2)/(1-\beta_0^2)};$$

and of the second one

$$\epsilon_{II}^{pp} = \frac{26_{pp}\omega_0^2}{\pi r_0^2 \ln\frac{1+\beta_0}{1-\beta_0}(1+2\beta_0)}, \qquad \epsilon_{II}^{a} = \frac{26_a \beta_0^2 \varepsilon_0^2}{\pi r_0^2(\sqrt{2}-1)(\beta_0^2+\sqrt{2})\ln\left(\frac{1+\beta_0}{1-\beta_0}\right)}$$

A.3. Simulation of Parameters of Field Photons.

It is assumed in calculations that the field photons are distributed isotropically. Then, the azimuth and zenith angles are sampled by formula

$$\cos\theta = 2r_1 - 1, \qquad \varphi = 2\pi r_2,$$

where r_1 and r_2 are random uniform numbers within the range (0.1).

In the case of power-law energy spectrum of field photons ($n(\omega) \sim \omega^{-\alpha}$; $\omega_1 \le \omega \le \omega_2$) the photon energy is sampled by formula

$$\omega = \left[r_1 \omega_2^{-\alpha+1} + (1-r_1)\omega_1^{-\alpha+1}\right]^{1/(1-\alpha)}$$

and in the case of blackbody radiation by formula [19]

$$\omega = -\kappa T_r \ln(r_1 r_2 r_3)/\eta ,$$

where η is the number defined by the condition

$$\eta = \begin{cases} 1 & 1{,}202\, r_4 < 1 \\ m & \sum_{j=1}^{m-1} j^{-3} < 1{,}202\, r_4 < \sum_{j=1}^{m} j^{-3} \quad , \quad m = 2,3,\ldots \end{cases}$$

It should be however noted that such an independent sampling of parameters of field photons is true only in the case of thresholdless reactions. In particular, for Compton scattering. But in the case of pair production process with the threshold $\omega^* = \frac{2}{E_\gamma (1-\cos\theta)}$ the simulation procedure is somewhat complicated. Thus for power-law spectra of field photons

$$\omega = \left[r_1 \omega_2^{-\alpha+1} + (1-r_1)\omega_m^{-\alpha+1} \right]^{1/(1-\alpha)}, \quad \omega_m = \max(\omega_1, \omega^*);$$

$$\cos\theta = 2 r_2 (1 - 1/E_\gamma \omega_2) - 1.$$

and in the case of blackbody radiation

$$\omega = \begin{cases} -\kappa T_r \ln(r_1 r_2 r_3)/\eta + \omega^* & \left[\frac{2\omega^*\eta}{\kappa T_r} + \left(\frac{\omega^*\eta}{\kappa T_r}\right)^2 \right]/M < r_4 < 1 \\ -\kappa T_r \ln(r_1 r_2)/\eta + \omega^* & \left(\frac{\omega^*\eta}{\kappa T_r}\right)^2/M < r_4 < \left[\frac{2\omega^*\eta}{\kappa T_r} + \left(\frac{\omega^*\eta}{\kappa T_r}\right)^2 \right]/M \\ -\kappa T_r \ln(r_1)/\eta + \omega^* & \left(\frac{\omega^*\eta}{\kappa T_r}\right)^2/M > r_4 \end{cases}$$

$$M = 2 + 2\frac{\omega^*\eta}{\kappa T_r} + \left(\frac{\omega^*\eta}{\kappa T_r}\right)^2 \quad \text{and} \quad \eta = K, \quad \text{if}$$

$$\sum_{j=1}^{K-1} M(j) < r_5/c_1 < \sum_{j=1}^{K} M(j) \; ; \qquad c_1 = 1 \Big/ \int_{\omega^*/\kappa T_r}^{\infty} x^2/(e^x - 1)\, dx \; ;$$

$$M(j) = j^{-3} \exp\left[-j\omega^*/\kappa T_r\right]\left[(j\omega^*/\kappa T_r)^2 + 2j\omega^*/\kappa T_r + 2\right].$$

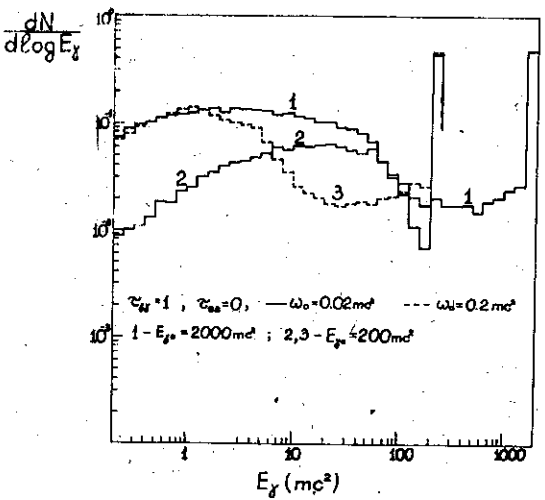
dN/dlogE_γ
τ_ii = 1 , τ_ee = 0 , —ω₀ = 0.02mc² --- ω₀ = 0.2mc²
1 - E_γ₀ = 2000mc² ; 2,3 - E_γ₀ = 200mc²
E_γ (mc²)

Fig.1a

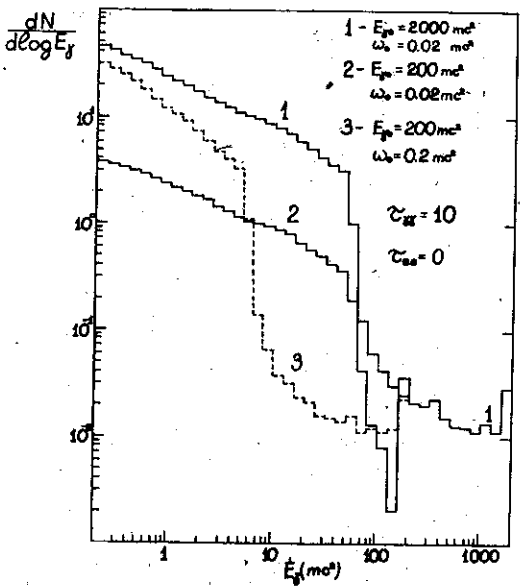
dN/dlogE_γ
1 - E_γ₀ = 2000 mc²
ω₀ = 0.02 mc²
2 - E_γ₀ = 200 mc²
ω₀ = 0.02mc²
3 - E_γ₀ = 200mc²
ω₀ = 0.2 mc²
τ_ii = 10
τ_ee = 0
E_γ (mc²)

Fig. 1b

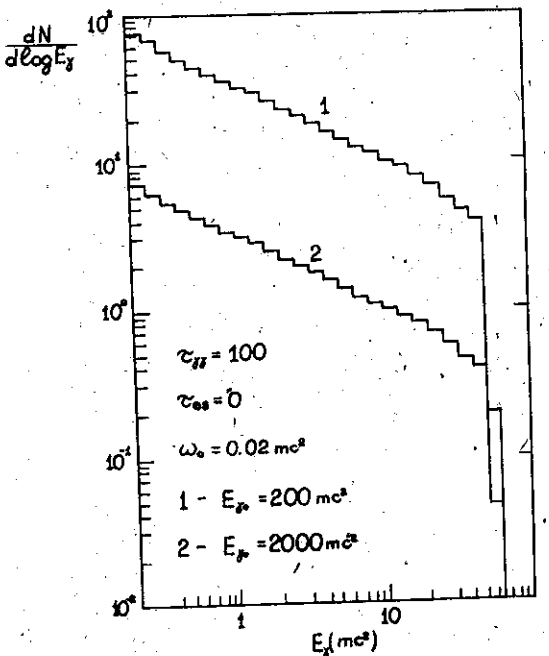
dN/dlogE_γ
10³
10²
10¹
10⁰
10⁻¹
10⁻²
1
10
E_γ(mc²)
1
2
τ_γγ = 100
τ_ee = 0
ω_o = 0.02 mc²
1 - E_p = 200 mc²
2 - E_p = 2000 mc²

Fig.1c

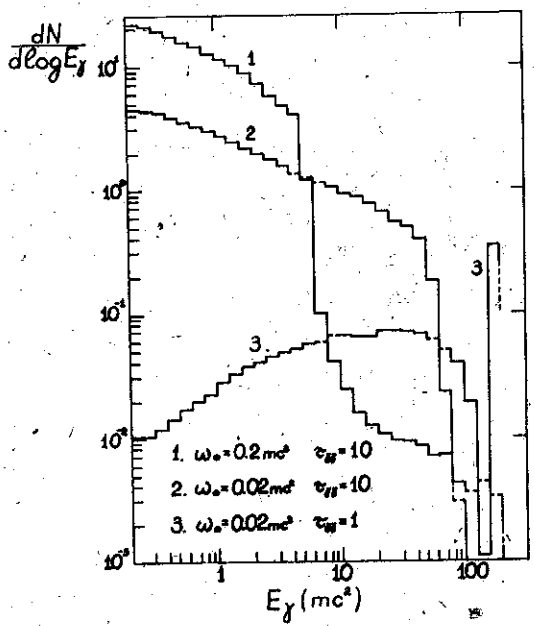
dN/dlogE_γ
10¹
10⁰
10⁻¹
10⁻²
10⁻³
1
10
100
E_γ(mc²)
1
2
3
1. ω_o = 0.2 mc² τ_γγ = 10
2. ω_o = 0.02 mc² τ_γγ = 10
3. ω_o = 0.02 mc² τ_γγ = 1

Fig. 2

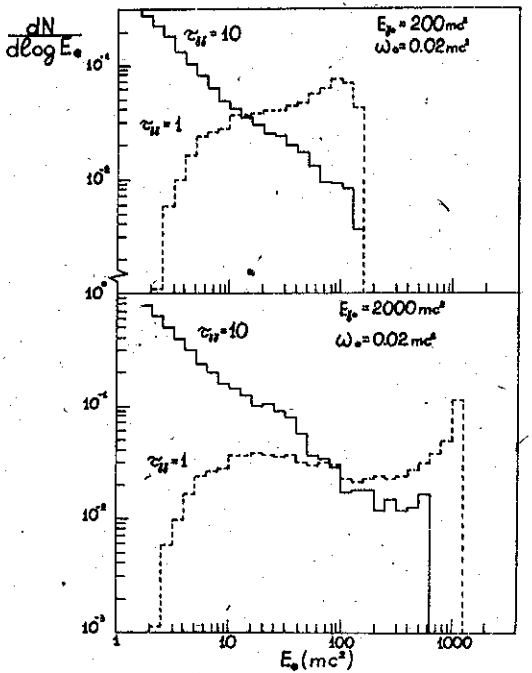
dN / d log E_e
τ_γγ = 10
E_γ₀ = 200 mc²
ω₀ = 0.02 mc²
τ_γγ = 1
E_γ₀ = 2000 mc²
ω₀ = 0.02 mc²
E_e (mc²)

Fig.3

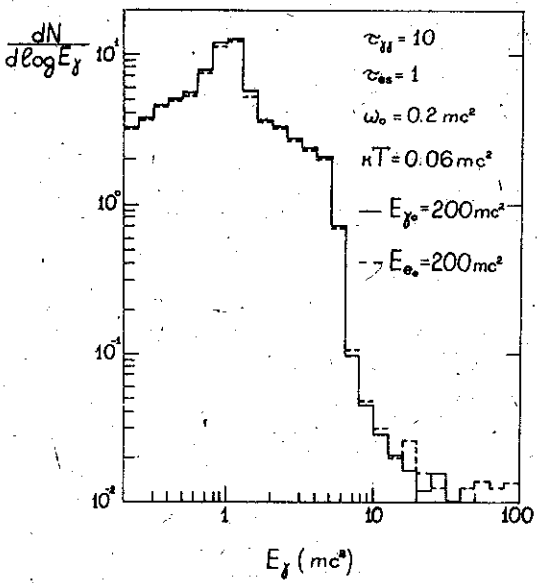
dN / d log E_γ
τ_γγ = 10
τ_ee = 1
ω₀ = 0.2 mc²
κT = 0.06 mc²
— E_γ₀ = 200 mc²
- - E_e₀ = 200 mc²
E_γ (mc²)

Fig.4

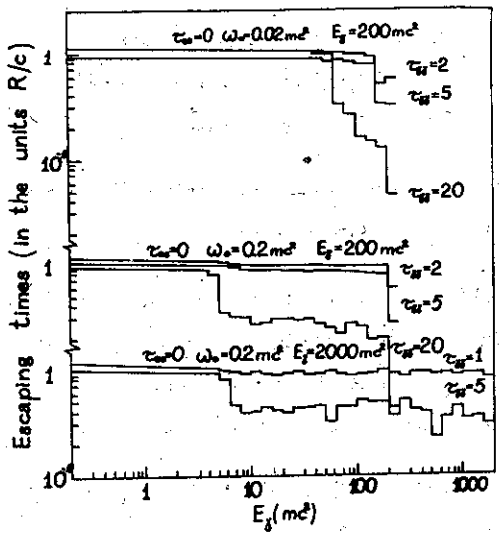
τ_{es}=0 ω_o=0.02mc² E_g=200mc²
τ_{es}=2
τ_{es}=5
τ_{es}=20
τ_{es}=0 ω_o=0.2mc² E_g=200mc²
τ_{es}=2
τ_{es}=5
τ_{es}=0 ω_o=0.2mc² E_g=2000mc²
τ_{es}=20
τ_{es}=1
τ_{es}=5
Escaping times (in the units R/c)
1
10
1
1
10
1
10
1
10
100
1000
E_g(mc²)

Fig.5

FIGURE CAPTIONS

Fig.1. Gamma-ray spectra escaping from the active region of cascade development per incident particle. The density of initiating cascade gamma-rays reduces by the radius as r^{-2} (Case I) a) $\tau_{es}=0$, $\tau_{\gamma\gamma}=1$; b) $\tau_{es}=0$, $\tau_{\gamma\gamma}=10$; c) $\tau_{es}=0$, $\tau_{\gamma\gamma}=100$

Fig.2. Escaping gamma-ray spectra per incident particle in the case of point source of initiating gamma-rays, located at the centre of spherical X-ray photon cloud (Case II).

Fig.3. The spectra of escaping electrons (positrons) per incident particle at $\tau_{es}=0$ in the Case I.

Fig.4. Escaping gamma-ray spectra per incident particle at $\tau_{\gamma\gamma}=10$ and $\tau_{es}=1$ in the Case I.

——— cascade initiated by gamma-rays;

------- cascade initiated by electrons.

Fig.5. Escaping times of photons in Case I (in the units R/c).

REFERENCES

1. Herterich K. Absorption of gamma-rays in intense X-ray sources. - Nature, 1978, vol.250, p.311.
2. Cavallo G., Rees M.J. A qualitative study of cosmic fireballs and γ-ray bursts. - MNRAS, 1978, vol.183, p.359.
3. Fabian A.C. Theories of the nuclei of active galaxies. - Proc. R. Soc. Lond., 1979, vol.366, p.449.
4. Aharonian F.A., Atoyan A.M., Nahapetian A.M. Photoproduction of electron-positron pairs in compact X-ray sources. - Astrofizika, 1983, vol.19, p.324.
5. Jones F.C. Calculated spectrum of inverse Compton scattered photons. - Phys.Rev., 1968, vol.167, p.1159.
6. Blumenthal G.R., Gould R.J. Bremsstrahlung, synchrotron radiation, and Compton scattering of high energy electrons traversing dilute gases. - Rev.Mod.Phys., 1970, vol.42, p.237.
7. Aharonian F.A., Atoyan A.M. Compton scattering of relativistic electrons in compact X-ray sources. - Astrophys. Space Sci., 1981, vol.79, p.321.
8. Aharonian F.A., Atoyan A.M. Cosmic gamma-rays associated with annihilation of relativistic e^+e^- pairs. - Phys. Letters, 1981, vol.83A, p.301.
9. Svensson R. The pair annihilation process in relativistic plasmas. - Ap. J., vol.256, p.321.
10. Akhiezer A.I., Berestetskii V.B. Quantum Electrodynamics. 1965, N.Y., Wiley.
11. Gould R.J., Schreder G.P. Pair production in photon-photon collisions. Phys.Rev., 1967, vol.155, p.1404.
12. Ginzburg V.L., Sirovatskii S.I. Origin of cosmic rays. 1964, N.Y., MacMilan.

13. Crannel C.J., Joyce G., Ramaty R., Werntz C. Formation of the 0.511 MeV line in solar flares. - Ap.J., 1976, vol.210, p.582.

14. Bussard R.W., Ramaty R., Drachman R.J. The annihilation of galactic positrons. - Ap. J., vol.228, p.928.

15. Aharonian F.A., Atoyan A.M., Sunyaev R.A. Radiation spectrum of optically thin relativistic electron-positron plasma. - Astrophys. Space Sci., 1983, vol.93, p.229.

16. Svensson R. The thermal pair annihilation spectrum: A detailed balance approach. - Ap. J., 1983, vol.270, p.300.

17. Messel H., Crawford D.F. Electron-photon shower function, 1970, Pergamon Press.

18. Burns M.L., Lovelace R.V.E. Theory of electron-positron showers in double radio sources. - Ap. J., 1982, vol.262, p.87.

19. Pozdnyakov L.A., Sobol I.M., Sunyaev R.A. In: "Astrophysics and Space Physics of Soviet Scientific Reviews", Ed. R.A.Sunyaev, 1982, N.Y., Harwood Academic Publishers.

The manuscript was received 19 July 1983

Ф.А.АГАРОНЯН, В.В.ВАРДАНЯН, В.Г.КИРИЛЛОВ-УГРЮМОВ

РАЗВИТИЕ ВЫСОКОЭНЕРГИЧНОГО ЭЛЕКТРОМАГНИТНОГО КАСКАДА, ИНИЦИИРУЕМОГО РЕЛЯТИВИСТСКИМИ ЭЛЕКТРОНАМИ И ГАММА-КВАНТАМИ В ГОРЯЧЕМ ФОТОННОМ ГАЗЕ

(на английском языке, перевод З.Н.Асланян)

Ереванский физический институт

Редактор Л.П.Мукаян

Тех.редактор А.С.Абрамян

Заказ 380 ВФ-05337 Тираж 299

Препринт ЕФИ Формат издания 60x84/16

Подписано к печати 8/XII-83г. 2,0 уч.-изд.л. Ц. 30 к.

Издано отделом научно-технической информации
Ереванского физического института, Ереван 36, Маркаряна 2

индекс 3624